

three equivalent positions around the hexagonal *c* axis (Baranov, Makarova, Muradyan, Tregubchenko, Shuvalov & Simonov, 1987; Merinov *et al.*, 1990). This implies that the H atom also jumps from one site to another, following the O(2) atom, *i.e.* one hydrogen bond breaks and another is formed. The transition at T_{c1} can thus be characterized as an order-disorder transition not only of hydrogen but also of the donor-oxygen atom in the hydrogen-bonded system.

In phase (II), where as stated earlier the space group is the same ($A2/a$) as that in the RT phase of the other members, all H atoms are disordered around the center of symmetry (see Fig. 2*a*). At the T_{c2} transition, half of the H atoms break hydrogen bonds and form alternative hydrogen bonds so as to form a dimer between two different adjacent selenate groups. As a result of this, non-H atoms shift their positions slightly, all atoms except O(1) lie in a mirror plane, and H atoms become disordered around a twofold axis in phase (III) (see Fig. 1). On passing through T_{c3} , the proton becomes ordered, as a result of which the twofold axis and the *C* base centering disappear and the primitive cell becomes doubled in phase (IV).

The authors wish to thank Mr Hilding Karlsson for his skilful technical assistance throughout this work. The work was partly supported by the International Scientific Program (Joint research) (63044002), and a Grant-in-Aid for Co-operative Research (02302021) from the Ministry of Education, Science and Culture, Japan, and a Grant-in-Aid from the Nippon Sheet Glass Foundation for Materials Science Research.

Acta Cryst. (1992). **B48**, 639–644

Electron Difference Density and Vibration Tensors in SrTiO₃

BY R. H. BUTTNER AND E. N. MASLEN

Department of Physics, University of Western Australia, Nedlands 6009, Australia

(Received 16 August 1991; accepted 21 April 1992)

Abstract

Multiple data sets for strontium titanate SrTiO₃: $M_r = 183.51$, cubic, $Pm\bar{3}m$, $a = 3.9092(4)$ Å, $V = 59.740(3)$ Å³, $Z = 1$, $D_x = 5.101$ Mg m⁻³, $\lambda(\text{Mo } K\alpha) = 0.71069$ Å, $\mu = 26.489$ mm⁻¹, $F(000) = 84$, $T = 298$ K, refinement indices range $R = 0.013$ – 0.028 ,

0108-7681/92/050639-06\$06.00

References

- BARANOV, A. I., MAKAROVA, I. P., MURADYAN, L. A., TREGUBCHENKO, A. V., SHUVALOV, L. A. & SIMONOV, V. I. (1987). *Sov. Phys. Crystallogr.* **32**, 400–407.
- BARANOV, A. I., MERINOV, B. V., TREGUBCHENKO, A. V., SHUVALOV, L. A. & SHCHAGINA, N. M. (1988). *Ferroelectrics*, **81**, 187–191.
- BARANOV, A. I., TREGUBCHENKO, A. V., SHUVALOV, L. A. & SHCHAGINA, N. M. (1987). *Sov. Phys. Solid State*, **29**, 1448–1449.
- GESI, K. (1980). *J. Phys. Soc. Jpn.* **48**, 886–889.
- ICHIKAWA, M. (1978). *Acta Cryst.* **B34**, 2074–2080.
- ICHIKAWA, M. (1987). *Acta Cryst.* **B43**, 23–28.
- ICHIKAWA, M. (1988). *J. Mol. Struct.* **177**, 441–448.
- ICHIKAWA, M., GUSTAFSSON, T. & OLOVSSON, I. (1991). *Solid State Commun.* **78**, 547–551.
- ICHIKAWA, M., GUSTAFSSON, T. & OLOVSSON, I. (1992). *Acta Cryst.* **C48**, 603–607.
- ICHIKAWA, M. & SATO, S. (1987). Unpublished work.
- JOHNSON, C. K. (1976). *ORTEPII*. Report ORNL-5138. Oak Ridge National Laboratory, Tennessee, USA.
- KOMUKAE, M., OSAKA, T., KANEKO, T. & MAKITA, Y. (1985). *J. Phys. Soc. Jpn.* **54**, 3401–3405.
- LEHMANN, M. S. & LARSEN, F. K. (1974). *Acta Cryst.* **A30**, 580–584.
- LUNDGREN, J.-O. (1983). *Crystallographic Computer Programs*. Report UUIC-B13-4-05. Institute of Chemistry, Univ. of Uppsala, Sweden.
- MCCANDLISH, L. E., STOUT, G. H. & ANDREWS, L. C. (1975). *Acta Cryst.* **A31**, 245–249.
- MERINOV, B. V., BARANOV, A. I. & SHUVALOV, L. A. (1990). *Sov. Phys. Crystallogr.* **35**, 200–203.
- MERINOV, B. V., BARANOV, A. I., TREGUBCHENKO, A. V. & SHUVALOV, L. A. (1988). *Sov. Phys. Dokl.* **33**, 715–716.
- MERINOV, B. V., BOLOTINA, N. B., BARANOV, A. I. & SHUVALOV, L. A. (1988). *Sov. Phys. Crystallogr.* **33**, 824–827.
- NODA, Y., WATANABE, Y., KASATANI, H., TERAUCHI, H. & GESI, K. (1991). *J. Phys. Soc. Jpn.* **60**, 1972–1977.
- OLOVSSON, I. & JÖNSSON, P.-G. (1976). *The Hydrogen Bond*, Vol. II, edited by P. SCHUSTER, G. ZUNDEL & C. SANDORFY, ch. 8. Amsterdam: North Holland.
- SAMSON, S., GOLDISH, E. & DICK, C. J. (1980). *J. Appl. Cryst.* **13**, 425–432.

$wR = 0.012$ – 0.028 for 91 unique reflections. Seven structure refinements from five different flux-grown crystals of SrTiO₃ are compared. The specimens selected showed mild to modest extinction. In all cases the mean-square vibration amplitude for the Ti atom along the Ti—O bond markedly exceeds that for the O atom. The amplitudes of the cations are

© 1992 International Union of Crystallography

low for the two data sets most affected by extinction. The atomic charges determined for these data sets are also outliers, but their values are not concordant with each other – a result attributable to the erratic extinction for the 011 reflection and its equivalents.

Introduction

The perovskite series with the ideal formula ABX_3 (Roth, 1957) includes several compounds with technological applications. The series is noted for its wide range of structural distortions and phase transitions, exemplified in the alkaline-earth titanates $ATiO_3$.

SrTiO₃, a well known substrate for thin-film preparations (Chen, Kwo & Hong, 1988), undergoes a phase transition from the ideal cubic $Pm\bar{3}m$ structure to tetragonal $I4/mcm$ at 106 K (Unoki & Sakudo, 1967) with further transitions to orthorhombic (65 K) and a possible rhombohedral structure below 35 K (Commercial Crystal Laboratories Inc., 1991). At a transition temperature between 0.2 and 0.3 K SrTiO₃ becomes superconducting (Schooley, Hosler & Cohen, 1964). It has been a test structure for modelling displacive transitions (Fleury, Scott & Worloch, 1968), in lattice dynamics (Stirling, 1972), and was studied spectroscopically by Barker & Tinkham (1962). The intensities of the stronger X-ray reflections from typical SrTiO₃ crystals are strongly attenuated by extinction, providing a test for extinction theories (*e.g.* Becker & Coppens, 1974, 1975; Hutton, Nemes & Scheel, 1981).

The electron density and vibration tensors in the archetypal cubic compounds KMF_3 , where M is a transition metal, were studied by several authors whose work was reviewed by Maslen & Spadaccini (1989). Maslen & Spadaccini (1992) recently suggested that the reliability of the extinction corrections limits the accuracy of measurements of the electron density in lattice-type structures. The degree of perfection in small single SrTiO₃ crystals prepared by flux growth varies. The consistency of electron densities measured from different samples provides an opportunity to check the reliability of both the densities and the extinction corrections – a desirable step if electron density studies are to deepen our understanding of the properties of matter.

Experimental

Small ($<0.001\text{ mm}^3$) well-faceted crystals of SrTiO₃ were prepared by the flux-growth method described by Sugi, Hasegawa & Ohara (1968). 10 g of $KF:KMnO_4:SrTiO_3$ in the molar ratio 60:30:10 was pressed into a pellet and heated in a 5 ml platinum crucible. To reduce the loss of flux this was capped with an inverted second crucible and the gap sealed

with a small amount of the mixture. After heating to 1473 K the sample was cooled at 15 K h^{-1} to 1246 K and at 30 K h^{-1} to room temperature. The volumes of the crystals released from the mixture by washing with nitric acid and water ranged from 10^{-5} to 10^{-2} mm^3 . The smaller specimens were transparent and apparently colourless, but the larger ones had a pale-yellow tinge characteristic of trace Fe impurities as reported by Scheel (1976).

Preliminary studies indicated that diffraction from many of the crystals was strongly attenuated by extinction, particularly for larger specimens. It is the norm for the intensities of strong Friedel-related reflections from SrTiO₃ crystals with a centrosymmetric habit to differ – indicating that the mosaic distribution in most crystals is not uniform, to a degree that varies from specimen to specimen.

Using five crystals differing in size and with varying but at most mild differences between Friedel equivalents seven data sets were measured at 298 K and refined. The measurements were made on a Syntex P_2 diffractometer with graphite-monochromatized $Mo\ K\alpha$ radiation ($\lambda = 0.71069\text{ \AA}$). Unit-cell dimensions were obtained from six equivalent $\{004\}$ reflections ($\sim 42.62 < 2\theta < 42.63^\circ$). Background measurements were made for one-third of the total time in an $\omega/2\theta$ scan at $4.88^\circ\text{ min}^{-1}$, $(\sin\theta/\lambda)_{\max} = 1.08\text{ \AA}^{-1}$, $-8 \leq h \leq 8$, $-8 \leq k \leq 8$, $-8 \leq l \leq 8$. Six standards (± 400 , ± 040 , ± 004) were measured every 100 reflections [± 033 replaced ± 004 in data set (1)]. Lorentz, polarization and absorption (Alcock, 1974) factors were corrected analytically. To first order each crystal's habit was determined by $\{100\}$ faces with dimensions listed in Table 1. Minor $\{110\}$ and $\{111\}$ face development, although included in the absorption calculations to improve the accuracy of the corrections for individual reflections, had little effect on the mean intensities averaged over the equivalent reflections, presumably because of the large number of equivalents for the cubic structure. The results of the analysis were also insensitive to modest ($\sim 3\text{ }\mu\text{m}$) changes to the dimensions for the $\{100\}$ faces. Variances in the measured structure factors from counting statistics were modified to allow for fluctuations of the primary beam intensity as indicated by the standards, and where necessary from comparison of equivalents using the Fisher test option in the program *SORTRF* (Hall & Stewart, 1989). The merging R_{int} values are higher than those for the KMF_3 perovskite data sets. There were pronounced (10–25%) discrepancies between the absorption-corrected intensities of equivalents for the strong 011 reflection for data sets (1), (2), (3), (4), (5) and (7), which could not be eliminated by physically reasonable adjustments to crystal shape. As this phenomenon was less marked for data set (6), measured with the smallest crystal, this was attributed to

Table 1. *Experimental and refinement data for SrTiO₃*

	Data set No.						
	(1)	(2)	(3)	(4)	(5)	(6)	(7)
<i>l</i> (± 100)*	37	46	52	52	52	10	32
<i>l</i> (0 ± 10)*	44	35	44	44	44	19	29
<i>l</i> (00 ± 1)*	27	35	27	27	27	41	28
<i>a</i> (Å)	3.911 (1)	3.9103 (8)	3.908 (3)	3.907 (3)	3.907 (3)	3.9092 (4)	3.911 (1)
<i>V</i> (Å ³)	59.822 (7)	59.790 (5)	59.68 (2)	59.63 (2)	59.63 (2)	59.740 (3)	59.822 (7)
<i>D_x</i> (Mg m ⁻³)	5.095	5.096	5.11	5.11	5.11	5.101	5.095
μ (mm ⁻¹)	26.466	25.463	26.520	26.534	26.534	26.489	26.466
Scan width (<i>a</i> + <i>b</i> tan θ) (°)	1.75, 0.70	1.75, 0.70	1.65, 0.70	1.65, 0.70	1.75, 0.70	2.00, 0.70	1.70, 0.70
Stability (standards)	0.013	0.006	0.008	0.005	0.014	0.017	0.015
No. of reflections measured	2691	2516	2516	3532	2726	2516	2549
Transmission range	0.18–0.35	0.18–0.28	0.09–0.20	0.09–0.20	0.09–0.20	0.37–0.60	0.25–0.34
<i>R_{int}</i> (initial)	0.149	0.059	0.112	0.114	0.118	0.106	0.073
<i>R_{int}</i> (absorption corrected)	0.105	0.039	0.077	0.081	0.079	0.037	0.079
<i>R</i>	0.020	0.013	0.015	0.028	0.017	0.015	0.028
<i>wR</i>	0.024	0.012	0.017	0.024	0.023	0.012	0.021
<i>S</i>	1.6 (1)	2.9 (2)	1.9 (2)	2.5 (2)	2.7 (2)	2.78 (1)	3.1 (2)
$\Delta\rho_{\max}$ (e Å ⁻³)	3.0 (2)	0.59 (7)	0.9 (1)	1.6 (1)	0.8 (1)	1.2 (1)	1.1 (1)
$\Delta\rho_{\min}$ (e Å ⁻³)	-1.4 (2)	-1.65 (7)	-2.1 (1)	-1.2 (1)	-2.0 (1)	-2.4 (1)	-3.1 (1)
<i>y_{min}</i> (extinction)	0.99	0.63	0.93	0.98	0.95	0.88	0.60

* *l* is the distance in μm from a common origin.Table 2. *Thermal parameters for SrTiO₃ ($U \times 10^5 \text{ \AA}^2$)*Temperature factor $T = \exp[-2\pi^2 a^{*2}(h^2 U_{11} + k^2 U_{22} + l^2 U_{33})]$.

	Data set No.						
	(1)	(2)	(3)	(4)	(5)	(6)	(7)
Sr ($U_{11} = U_{22} = U_{33}$)	680 (14)	617 (13)	710 (10)	643 (12)	669 (14)	683 (13)	580 (21)
Ti ($U_{11} = U_{22} = U_{33}$)	547 (12)	503 (9)	575 (10)	533 (13)	535 (14)	514 (11)	416 (13)
O (U_{11})	336 (58)	274 (42)	295 (39)	315 (59)	293 (63)	362 (60)	235 (60)
O ($U_{22} = U_{33}$)	924 (43)	957 (31)	913 (28)	858 (38)	878 (44)	975 (42)	869 (44)

secondary extinction. Atomic form factors and the dispersion correction cross-sections were taken from *International Tables for X-ray Crystallography* (1974, Vol. IV). Refinement weights $w = 1/\sigma^2(F_o)$ applied for all 91 independent reflections. That is, in accord with good statistical practice, no reflections were classified arbitrarily as 'unobserved'. Least-squares residual $\sum w|F_o - F_c|^2$ minimized by adjusting one scale and the four independent vibrational parameters, along with r^* in the Zachariasen (1969) isotropic secondary-extinction corrections

$$y = (1 + 2x)^{-1/2} = (1 + 2r^*F_k^2Q)^{-1/2},$$

where for unpolarized X-rays

$$Q = (e^4/m^2c^4V^2)(\lambda^3/\sin 2\theta) \times [(1 + \cos^4 2\theta)/(1 + \cos^2 2\theta)]\bar{T},$$

following the notation of Larson (1970). Final shift/e.s.d. < 0.0001. Other experimental and refinement details are listed in Table 1.† Computer programs *STARTX*, *DIFDAT*, *ABSORB*, *ADDTM*, *ADDREF*, *FC*, *SFLSX*, *BONDLA*, *FOURR*,

† A list of structure factors for data set (5) has been deposited with the British Library Document Supply Centre as Supplementary Publication No. SUP 55165 (3 pp.). Copies may be obtained through The Technical Editor, International Union of Crystallography, 5 Abbey Square, Chester CH1 2HU, England.

CHARGE, *CONTRS*, *SLANT* and *PLOT* from the *XTAL2.6* system (Hall & Stewart, 1989) installed on a SUN 280 computer, were used in the analysis. Anisotropic vibration parameters, listed in Table 2, are significantly below the mean for the cations in data sets (2) and (7), which are affected more strongly by extinction than data sets (1), (3), (4), (5) and (6). This may indicate that extinction could be better described with the Zachariasen (1969) expression modified by a $\sin\theta$ -dependent term resembling a temperature factor. Alternatively, it may reflect the increasing inaccuracy of the perturbation expansion underlying that expression as the extinction correction deviates further from unity.

Atomic charges

Atomic charges, determined by projecting the electron difference density onto atomic density basis functions following the method of Hirshfeld (1977) are listed in Table 3. The values for data sets (1), (3), (4) and (5) with modest extinction are broadly consistent. The outlying extinction-affected data sets (2) and (7) correspond to the least and most polar charge determinations respectively. The small charges for data set (2), indicated by the reliability indices to be the most accurate, reflect a trend reported by Maslen & Spadaccini (1992), *i.e.* extinc-

Table 3. Atomic charges (e)

	Data set No.						
	(1)	(2)	(3)	(4)	(5)	(6)	(7)
Sr	1.0 (1)	0.41 (4)	0.95 (8)	0.91 (8)	0.90 (7)	0.59 (6)	1.74 (9)
Ti	0.5 (1)	-0.02 (4)	1.16 (8)	0.91 (7)	0.78 (6)	0.29 (6)	1.47 (8)
O	-0.5 (1)	-0.13 (2)	-0.70 (8)	-0.61 (9)	-0.56 (8)	-0.30 (4)	-1.1 (1)

tion determined by minimizing F_o versus F_c discrepancies can erroneously reduce polarity for structures containing cations heavier than the anions.

In that context the strong polarity indicated by the data set (7) analysis appears anomalous. Test calculations showed that the anomaly is related to the strong 011 reflection for which the intensity measurements of equivalents for this data set were erratic. With its multiplicity of 12 the residual of this reflection, with values -0.16 and -2.88 e for data sets (2) and (7) respectively, strongly influences the polarity measured for this structure. The $F_o - F_c$ values for this reflection for the less strongly extinction-affected data sets (1), (3), (4), (5) and (6), range from -0.65 to -1.42 e. The inconsistency in the intensities measured for this extinction-affected structure factor is thus responsible for the wide range of polarities observed.

The crystal for data set (6) was an elongated prism. A comparison of the intensities measured for the stronger intensities as a function of path length confirmed that the effects of extinction for this crystal were small. The charges determined for a structure refinement without extinction correction of 1.06 (6), 0.97 (6) and -0.68 (4) e for Sr, Ti and O respectively are closer to the results for sets (1), (3), (4) and (5) than are the data set (6) values given in Table 3. Although the extinction in this structure is not severe enough to cause a breakdown of the perturbation expression for the extinction corrections, it appears unlikely that those corrections have been determined accurately. The limitations of the method for determining extinction corrections used in this analysis are addressed by Maslen & Spadaccini (1992).

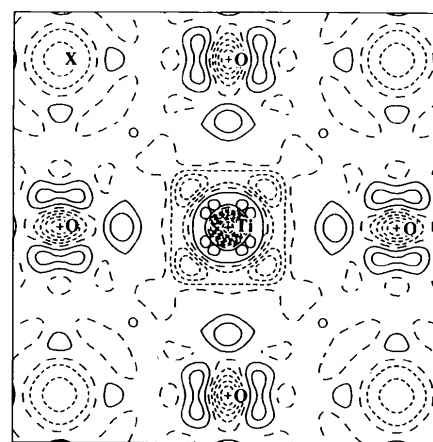
Structural parameters

The structural geometry of SrTiO₃ is isomorphic with those of the cubic KMF_3 perovskites. With Ti at the cell origin and Sr at the centre there are O atoms at the centres of all cell edges.

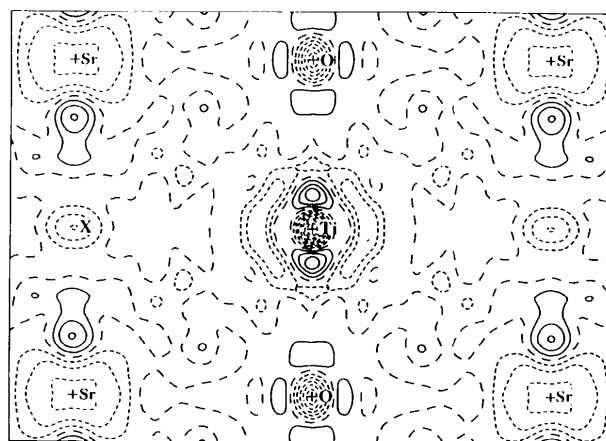
The U_{11} value for O, corresponding to motion along the Ti—O bond, is 0.002 \AA^2 less than that of the Ti atom, in marked contrast with the behaviour in the KMF_3 series, where U_{11} for F typically exceeds that of M by 0.0001 \AA^2 . Error in the experimental measurements can be excluded as a cause, because the same phenomenon is observed for all data sets. Larger anion amplitudes are more common for

strong cation-anion interactions, for which bond-stretch amplitudes are small, and the motions for light atoms are larger than those for heavy cations.

Scott (1974) pointed out the near ferroelectric nature of SrTiO₃, substitution of Sr by only a small percentage of Ba being enough to induce a ferroelectric transition. The large difference between the U_{11} values for O and Ti along the Ti—O bond assumes high significance, because a large Ti—O vibration amplitude implies that SrTiO₃ is to some extent dynamically unstable. That is, the large vibrational



(a)



(b)

Fig. 1. $\Delta\rho$ for SrTiO₃, data set (5): (a) (100) plane, map borders $5.0 \times 5.0 \text{ \AA}$; (b) (011) plane, map borders $7.0 \times 5.0 \text{ \AA}$. Contour intervals 0.25 \AA^{-3} , positive, zero and negative contours - solid, long and short dashes respectively.

amplitude for Ti is the counterpart in SrTiO₃ of the static displacement of the Ti atom responsible for the ferroelectric properties of BaTiO₃. Mild doping of Sr with Ba changes the equilibrium from the dynamically unstable ideal structure to the tetragonally distorted structure with Ti displaced from the ideal position.

It is difficult to understand that phenomenon on the basis of the ideal atomic model for SrTiO₃ with Sr and Ti having electron configurations $1s^2 2s^2 2p^6 3s^2 3p^6 3d^{10} 4s^2 4p^6 5s^2$ and $1s^2 2s^2 2p^6 3s^2 3p^6 3d^2 4s^2$ respectively. In this context a reduced population of the 3d subshell for Ti would be important. In the ionic model that population for a Ti⁴⁺ ion would be zero, but it is difficult to reconcile a two-electron reduction in the 3d subshell population with the charges in Table 3. The lesser reduction to a one-electron occupation of the 3d subshell suggested by the charges in Table 3 would result in a dynamically unstable system due to the

degeneracy of the 3d¹ state. This follows from the Jahn–Teller (Jahn & Teller, 1937) theorem, which states that for an octahedral field the degeneracy of a 3d¹ state would be removed by small perturbations to the system, lowering the symmetry. It is well known that thermal parameters tend to be higher for Jahn–Teller systems. For Ti in SrTiO₃ the effect must be small since the average symmetry is maintained. Nevertheless this is relevant when assessing the thermal parameters listed in Table 2.

Difference density

Difference densities for the (001) and (011) planes for data set (5) are depicted in Figs. 1(a) and 1(b). The degree of consistency with those for the other data sets can be gauged by comparing Fig. 1(b) with Figs. 2(a) and 2(b), the difference densities in the (011) plane for data sets (2) and (3) respectively. The difference density for data set (2) differs strongly from those for data sets (3), (4) and (5) near the nucleus position, as expected because that data set is affected strongly by extinction. The quality of data set (4) is degraded slightly compared with the remainder due to a minor equipment malfunction. The distribution of errors among the structure factors is most nearly uniform for data sets (3) and (5), for which the difference densities show the highest degree of correspondence. The density maps for data set (5) shown in Fig. 1 closely resemble those in the electron difference density for BaTiO₃ (Buttner, 1990).

The mild degree of anisotropy of the density near the Ti nucleus in these maps is consistent with that expected for a 3d subshell which is lightly populated. The distribution near the Sr nucleus is somewhat more anisotropic than that near Ti, as would be expected if there is some electron transfer from the 5s subshell to the 4d subshell for this atom. There is a marked depletion of electron density at the structural cavity midway between the Sr atoms, similar to that which occurs for some members of the KMF₃ series (Maslen & Spadaccini, 1989).

The contributions of computer programs by their authors R. Alden, G. Davenport, R. Doherty, W. Dreissig, H. D. Flack, S. R. Hall, J. R. Holden, A. Imerito, R. Merom, R. Olthof-Hazekamp, M. A. Spackman, N. Spadaccini and J. M. Stewart to the XTAL2.6 system (Hall & Stewart, 1989), used extensively in this work, is gratefully acknowledged. This research was supported by the Australian Research Council.

References

- ALCOCK, N. W. (1974). *Acta Cryst.* **A30**, 332–335.
BARKER, A. S. & TINKHAM, M. (1962). *Phys. Rev.* **125**, 1527–1530.

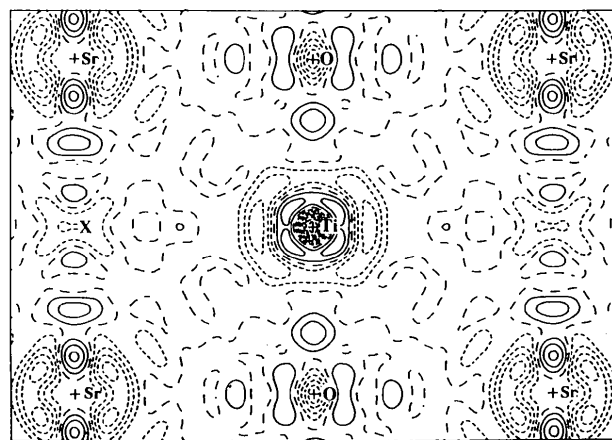
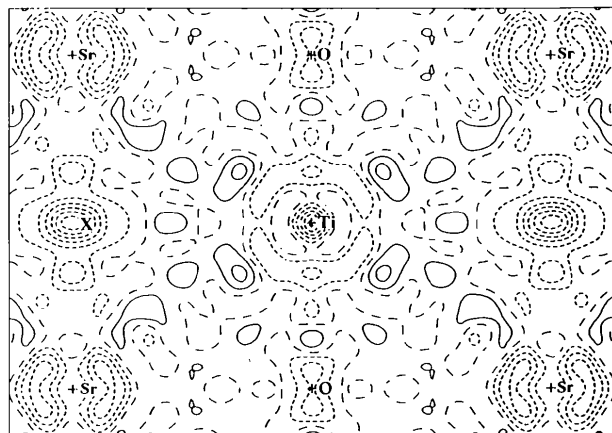


Fig. 2. $\Delta\rho$ for SrTiO₃, (011) plane, map borders 7.0×5.0 Å: (a) data set (2), (b) data set (3). Contouring as in Fig. 1.

- BECKER, P. J. & COPPENS, P. (1974). *Acta Cryst.* **A30**, 129–147.
 BECKER, P. J. & COPPENS, P. (1975). *Acta Cryst.* **A31**, 417–425.
 BUTTNER, R. H. (1990). PhD thesis, Univ. of Western Australia, Australia.
 CHEN, C. H., KWO, J. & HONG, M. (1988). *Appl. Phys. Lett.* **52**, 841–843.
 Commercial Crystal Laboratories Inc. (1991). *Physical Properties of Strontium Titanate*, Company Circular No. 3.
 FLEURY, P. A., SCOTT, J. F. & WORLOCK, J. A. (1968). *Phys. Rev. Lett.* **21**, 16–19.
 HALL, S. R. & STEWART, J. M. (1989). Editors. *XTAL2.6 Users Manual*. Univ. of Western Australia, Australia, and Maryland, USA.
 HIRSHFELD, F. L. (1977). *Isr. J. Chem.* **16**, 198–201.
 HUTTON, J., NELMES, R. J. & SCHEEL, H. J. (1981). *Acta Cryst.* **A37**, 917–920.
 JAHN, H. A. & TELLER, E. (1937). *Proc. R. Soc. London Ser. A*, **161**, 220–235.
 LARSON, A. C. (1970). In *Crystallographic Computing*, edited by F. R. AHMED. Copenhagen: Munksgaard.
 MASLEN, E. N. & SPADACCINI, N. (1989). *Acta Cryst.* **B45**, 45–52.
 MASLEN, E. N. & SPADACCINI, N. (1992). In preparation.
 ROTH, R. S. (1957). *J. Res. Natl Bur. Stand.* **58**, 75–88.
 SCHEEL, H. J. (1976). *Z. Kristallogr.* **143**, 417–428.
 SCHOOLEY, J. F., HOSLER, W. R. & COHEN, M. L. (1964). *Phys. Rev. Lett.* **14**, 474–475.
 SCOTT, J. F. (1974). *Rev. Mod. Phys.* **46**, 86–128.
 STIRLING, W. G. (1972). *J. Phys. C*, **5**, 2711–2730.
 SUGI, T., HASEGAWA, S. & OHARA, G. (1968). *Jpn. J. Appl. Phys.* **7**, 358–362.
 UNOKI, H. & SAKUDO, T. (1967). *J. Phys. Soc. Jpn.* **23**, 546–552.
 ZACHARIASEN, W. H. (1969). *Acta Cryst.* **A25**, 102.

Acta Cryst. (1992). **B48**, 644–649

Electron Difference Density and Structural Parameters in CaTiO₃

BY R. H. BUTTNER AND E. N. MASLEN

Department of Physics, University of Western Australia, Nedlands 6009, Australia

(Received 16 August 1991; accepted 22 April 1992)

Abstract

Calcium titanate, CaTiO₃, $M_r = 135.98$, orthorhombic, $Pbnm$, $a = 5.388$ (1), $b = 5.447$ (1), $c = 7.654$ (1) Å, $V = 224.63$ (1) Å³, $Z = 4$, $D_x = 4.02$ Mg m⁻³, $\lambda(\text{Mo } K\alpha) = 0.71069$ Å, $\mu = 5.778$ mm⁻¹, $F(000) = 264$, $T = 298$ K, $R = 0.043$, $wR = 0.028$ for data set (1) and $R = 0.037$, $wR = 0.026$ for data set (2) for 1240 and 1241 unique reflections respectively. Structural parameters and difference electron densities for CaTiO₃ were determined from two sets of X-ray diffraction data measured independently. There was close agreement between the analyses. The topography of $\Delta\rho$ near the Ti atom resembles that frequently observed for d^8 or d^9 systems, with a change of sign, indicating that its 3d subshell is partly filled. There are indications of slight Jahn–Teller distortion in the structural geometry, in the vibration parameters and in the electron density.

Introduction

The first perovskite mineral CaTiO₃ was assigned that name by Gustav Rose in 1830 (Hazen, 1988). Naray-Szabo (1943) determined its structure to be monoclinic but Megaw (1946) pointed out that an orthorhombic cell could be derived from the monoclinic lattice. Single-crystal structure analysis by Kay & Bailey (1957) confirmed the orthorhombic cell, having space group $Pcmm$. The volume of the ortho-

rhombic cell is approximately four times that of an ideal cubic perovskite ($Pm\bar{3}m$ symmetry), and is analogous to tetragonal KCuF₃ (Buttner, Maslen & Spadaccini, 1990). Structural parameters for CaTiO₃ have been determined accurately by Sasaki, Prewitt, Bass & Schulze (1987).

The electron distributions for ideal cubic KMF_3 perovskites with $M = \text{Mn, Fe, Co, Ni}$ and Zn have been studied by Kijima, Tanaka & Marumo (1981, 1983), by Miyata, Tanaka & Marumo (1983) and by Buttner & Maslen (1988). The effect of Jahn–Teller (Jahn & Teller, 1937) distortion of the M atom was examined by Buttner, Maslen & Spadaccini (1990), their results for KCuF₃ being broadly consistent with those re-derived from earlier data by Tanaka & Marumo (1982). These studies of the perovskites are now extended to CaTiO₃, and thus to the effect on the electron density of structural distortions due to the atomic radii differing from the ideal cubic structure values.

Experimental

Crystals were prepared by the flux-growth method used by Sugi, Hasegawa & Ohara (1968) to crystallize SrTiO₃. 10 g of a mixture of KF:KMoO₄:CaTiO₃ in the molar ratio 60:30:10 was pressed into a pellet and placed in a platinum crucible with a small quantity of the mixture sealing the gap to a capping crucible. The assembly was heated to 1323 K and